Topochemical Control in the Solid-State Conversion of Cyclotrigallazane into Nanocrystalline Gallium Nitride

Jen-Wei Hwang, John P. Campbell, Jan Kozubowski, Scott A. Hanson, John F. Evans, and Wayne L. Gladfelter*

Department of Chemistry and the Center for Interfacial Engineering, University of Minnesota, Minneapolis, Minnesota 55455

Received September 7, 1994. Revised Manuscript Received December 12, 1994[⊗]

Pyrolysis of powdered samples of cyclotrigallazane, $[H_2GaNH_2]_3$, under a variety of conditions led to nanocrystalline gallium nitride. Thermogravimetric analysis established that the primary weight loss event occurred at 150 °C and mass spectral analysis verified the production of hydrogen with lesser amounts of ammonia. The final weight in the TGA experiments (achieved above 500 °C) and the elemental analyses established that the formula of the powder was $GaN_{0.83}$. Transmission electron microscopy (TEM) and X-ray line broadening established that the particles were approximately 60 Å in diameter, and high-resolution TEM measurements revealed lattice fringes in the images. Modeling the X-ray diffraction data using the Debye equation established that the nanocrystalline GaN had neither the pure wurtzite nor the pure zinc blende structure. The best fit to the data was found for a random arrangement of stacking planes with an equal amount of cubic and hexagonal planes. The nanocrystalline material slowly converted into the known wurtzite phase at 900 °C. Synthesis of bulk GaN at 600 °C from Ga_2O_3 and NH_3 produced only the pure wurtzite phase. The synthesis of metastable samples of gallium nitride comprised of such a high percentage of the cubic phase was proposed to result from a topochemical reaction in which the hydrogen elimination (with concomitant Ga–N bond formation) occurs along a reaction coordinate established by the crystal and molecular structure of $[H_2GaNH_2]_3$.

Introduction

There is much interest in developing new synthetic methods for preparing solid-state compounds with the expectation that improved processing conditions (e.g., lower temperatures), better products (e.g., higher purity), or new materials will result. A growing number of examples are appearing which strongly suggest a relationship can exist between the structures of the molecular precursor and the solid-state product.[1–4]

The technologically significant compound semiconductors have two common structures, zinc blende (cubic) and wurtzite (hexagonal). Among the III–V semiconductors, only the nitrides of aluminum, gallium, and indium exhibit the wurtzite structure, and under typical conditions the alternative phase is not known for any of the III–V compounds. This behavior sharply contrasts that found among the II–VI semiconductors. Not only do compounds such as ZnS and CdSe exist in both the zinc blende and wurtzite lattices, but polytypism yields a gradation between the two end members.[5,6]

This paper focuses on a molecular route to gallium nitride which is a wide-bandgap semiconductor (3.5 eV) of interest for use in various optoelectronic devices. The molecular precursor cyclotrigallazane,[1] ($[H_2GaNH_2]_3$, **1**)

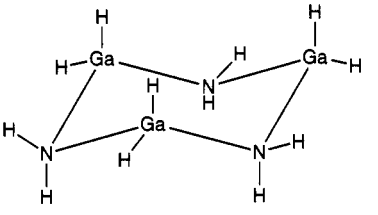

1

is the fully characterized, parent member (no organic groups) of a structurally diverse class of compounds comprised of clusters of mono- and diorganogallium and NH and/or NH_2 (and their corresponding organonitrogen counterparts) moieties. The lack of any organic substituents made cyclotrigallazane a prime candidate for generating carbon-free gallium nitride.

Known preparations of bulk samples of hexagonal GaN include the reactions shown in eqs 1–3:[7–9]

$$Ga_2O_3 + 2NH_3 \rightarrow 2GaN + 3H_2O \quad (1)$$

$$Ga + NH_3 \rightarrow GaN + {}^3/_2H_2 \quad (2)$$

$$[NH_4][GaF_6] + NH_3 \rightarrow GaN + HF \quad (3)$$

Thin films of hexagonal (and rarely cubic) GaN can be

[⊗] Abstract published in *Advance ACS Abstracts,* January 15, 1995.

(1) Hwang, J.-W.; Hanson, S. A.; Britton, D.; Evans, J. F.; Jensen, K. F.; Gladfelter, W. L. *Chem. Mater.* **1990**, *2*, 342.
(2) Banazsak Holl, M. M.; Wolczanski, P. T.; Van Duyne, G. D. *J. Am. Chem. Soc.* **1990**, *112*, 7989.
(3) MacInnes, A. N.; Power, M. B.; Barron, A. R. *Chem. Mater.* **1993**, *5*, 1344.
(4) Hessen, B.; Siegrist, T.; Palstra, T.; Tanzler, S. M.; Steigerwald, M. L. *Inorg. Chem.* **1993**, *32*, 5165.
(5) Verma, A. R.; Krishna, P. *Polymorphism and Polytypism in Crystals*; Wiley: New York, 1966; p 341.
(6) Trigunayat, G. C. *Solid State Ionics* **1991**, *48*, 3.
(7) Schoonmaker, R. C.; Burton, C. E. *Inorg. Synth.* **1963**, *7*, 16.
(8) Johnson, W. C.; Parsons, J. B.; Crew, M. C. *J. Phys. Chem.* **1932**, *36*, 2651.
(9) Juza, R.; Hahn, H. *Z. Anorg. Allg. Chem.* **1940**, *244*, 111.

0897-4756/95/2807-0517$09.00/0

prepared using the reactions shown in eqs 4–6:[10–12]

$$GaMe_3 + NH_3 \rightarrow GaN + 3CH_4 \quad (4)$$

$$GaMe_3 + N_2H_4 \rightarrow GaN + CH_4 \quad (5)$$

$$Ga(atoms) + N(atoms) \rightarrow GaN \quad (6)$$

Experimental Section

Cyclotrigallazane, $[H_2GaNH_2]_3$, was prepared following the literature method.[1] Ammonia (Matheson) and β-gallium oxide (Alfa) were used as received. X-ray powder diffraction studies were conducted using a Seimens D500 diffractometer with monochromatic (graphite) Cu Kα radiation. Elemental analyses were done by Galbraith Laboratories, Knoxville, TN.

Pyrolysis of Cyclotrigallazane. The apparatus consisted of a quartz tube (2.5 cm i.d.) which was sealed at one end and which was connected to a stopcock via a 29/42 ground glass joint. The other end of the stopcock was fitted with a Tee which was connected to a source of argon, nitrogen, or ammonia and a mineral oil bubbler. In a glovebox, the sample was loaded into a quartz boat which was placed into the reaction tube. After the valve was attached and closed, the loaded quartz tube was placed in a tube furnace and connected to the desired gas. After the lines were flushed with the desired gas, the valve was opened. An Omega temperature controller was used to maintain the desired temperature. The thermocouple was located between the furnace and the quartz tube at the same position as the sample. After the system reached the desired temperature, it was heated for a preset period of time and then cooled under the same atmosphere. The powder changed color from white to gray or black during the pyrolysis. For a sample treated at 600 °C under argon; Anal. Calcd for $GaN_{1.00}$: Ga, 83.27; N, 16.73. Found: Ga, 85.99; N, 14.31; H, <0.5; C, <0.5. On a sample independently produced under the same conditions the percent nitrogen was found to be 14.18.

Pyrolysis of Cyclotrigallazane at High Pressure. A small Pd tube (5 mm o.d. < 1 mm wall thickness) was flame welded at one end then cut into a length of 2.5 cm. In a glovebox, the tube was charged with gallazane (approximately 50 mg) and crimped. The tube was removed from the glovebox and flame welded. The tube was then placed into a high-pressure chamber which was purged with argon then pressurized to 3 kbar. The temperature was raised to 600 °C and maintained for 4 h. After cooling, the pressure was released and the tube was cut open. The black solid was removed and characterized.

Thermogravimetric Analysis. All thermogravimetric measurements were done by Thermal Options, Escondido, CA. Experiments were carried out under 80 sccm flowing argon with a 20 °C/min heating rate. A total of three samples were examined. In a typical experiment, an ampule containing the sample was opened and quickly transferred into a platinum or a ceramic pan which served as the sample stage under argon atmosphere. Sample sizes ranged between 12 and 24 mg. Cyclotrigallazane apparently corroded the platinum since a 5 mm hole was observed at the end of the analysis. Despite this, the results were comparable with that when a ceramic pan was used.

Temperature-Programmed Mass Spectroscopy. The experiment was performed in a stainless steel, six-way cross appended to a diffusion-pumped chamber (base pressure = 6×10^{-9} Torr) containing an Extranuclear 8 in. quadrupole mass spectrometer. Under a nitrogen purge, $[H_2GaNH_2]_3$ was placed on a heating stage in the six-way cross. The system was sealed and pumped down to ca. 1×10^{-8} Torr, and a background spectrum was acquired. The heating stage was warmed at a rate of ca. 1 °C/s while continuously monitoring the mass spectrum of the gases evolved. The background spectrum was subtracted from the spectra obtained during heating.

Chemical Vapor Deposition. The apparatus was similar to that used for the solid-state pyrolysis. Cyclotrigallazane was placed at the sealed end of the quartz tube. Due to the involatility of $[H_2GaNH_2]_3$, this portion of the tube also required heating. This was accomplished either by wrapping the tube with heating tape or by inserting it into an oven. The temperature used to induce sublimation was approximately 45 °C. The substrates (Si (100) wafers) were placed upright ca. 8–15 cm from the sealed end. The temperature of the tube near the center of the furnace was raised to 650 °C. Although the first wafer was coated with a gray, powdery material, the second wafer was coated with a smooth film (4000 Å). The other two wafers were coated with much thinner films (1600 Å). The films were analyzed using X-ray diffraction.

Gallium Nitride from the Ammonolysis of Gallium Oxide. In the same apparatus described for the pyrolysis of cyclotrigallazane, Ga_2O_3 (0.9373 g, 5 mmol) was heated under ammonia at 600 °C for 41 h. On the basis of the weight loss (0.0143 gm), a 14% conversion to a light yellow powder was achieved. Following grinding, additional heating for 141 h (182 h total) under ammonia resulted in 30% conversion. Final heating, after regrinding, for 123 h (305 h total) resulted in a 84% conversion of Ga_2O_3 to *h*-GaN (0.7216 g).

Phase Transition from *c*/*h*-GaN to *h*-GaN. Nanocrystalline gallium nitride prepared from the pyrolysis of cyclotrigallazane at 600 °C under argon was heated to 900 °C. The progress of the transition was monitored using X-ray powder diffraction.

Transmission Electron Microscopy and Electron Diffraction of the GaN Powder. Specimens for TEM study were pulverized in an agate mortar. The resulting powder was dispersed in water and deposited on carbon-coated grids. All studies were conducted using a Philips CM30 TEM operating at 300 kV.

Modeling X-ray Diffraction Data for Nanocrystalline GaN. We have obtained a copy of the code used by Bawendi et al.[13] to model X-ray scattering in nanocrystalline CdSe and have modified it to model GaN as well as to run on the Cray X-MP and the Cray-2 at the Minnesota Supercomputer Center (MSC). The code requires that the lattice parameter, a, the cluster radius, the stacking sequence, the thermal factor, the starting and ending 2θ, and the step size be input. It generates a table of atomic positions to be used by the main part of the program. The main program calculates the X-ray diffraction pattern. The GaN crystallites are very small, approximately 60 Å in diameter, allowing use of the Debye equation for calculating the coherent scattering of X-rays:[14]

$$f(q) = \sum_i \sum_j F_i(q)\, F_j(q)\, \sin(qr_{ij})/qr_{ij} \quad (7)$$

where $f(q)$ is the coherently scattered intensity, $F_i(q)$ and the $F_j(q)$ are the structure factors for Ga and N, r_{ij} is the distance between atoms i and j, and $q = \sin\theta/\lambda$. The summation is taken over all i and j, where i and j run over all the atoms in the cluster; approximately 10 000 atoms for a 60 Å cluster. The calculated intensity is corrected for temperature with a Debye–Waller factor. Form factors $F(q)$ are taken from standard tabulated values for Ga and N.[15]

Results

Pyrolysis and Characterization of the Reaction and Products. Heating white, microcrystalline powder of $[H_2GaNH_2]_3$ yielded a dark gray to black powder. A

(10) Mizuta, M.; Fujieda, S.; Matsumoto, Y.; Kawamura, T. *Jpn. J. Appl. Phys.* **1986**, *25*, L945.
(11) Paisley, M. J.; Sitar, Z.; Posthill, J. B.; Davis, R. F. *J. Vac. Sci. Technol.* **1989**, *A7*, 701.
(12) Powell, R. C.; Tomasch, G. A.; Kim, Y. W.; Thornton, J. A.; Greene, J. E. In *Fall Meeting*; Materials Research Society: Pittsburgh, PA, 1989.
(13) Bawendi, M. G.; Kortan, A. R.; Steigerwald, M. L.; Brus, L. E. *J. Chem. Phys.* **1989**, *91*, 7282.
(14) Guinier, A. *X-Ray Diffraction in Crystals, Imperfect Crystals, and Amorphous Bodies*; Freeman: San Francisco, 1963; p 378.
(15) Cromer, D. T.; Mann, J. B. *Acta Crystallogr.* **1968**, *A24*, 321.

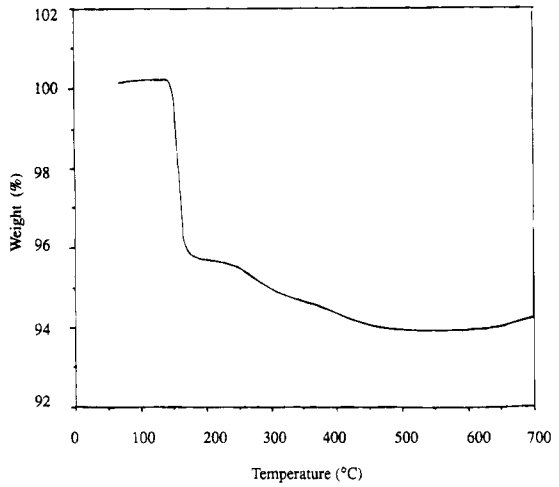

Figure 1. Thermogravimetric analysis of cyclotrigallazane. The heating rate was 20 °C/min.

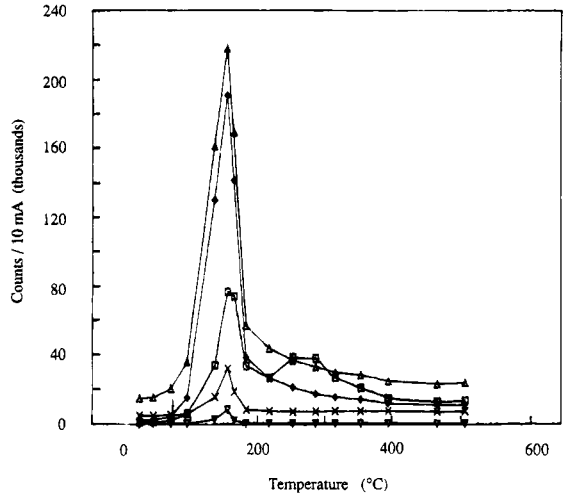

Figure 2. Mass spectral analysis of the gases evolved during a temperature-programmed decomposition of cyclotrigallazane. Mass (species): ▲ = 17 (NH_3), ◇ = 16 (NH_3), □ = 2 (H_2), × = 28 (N_2), ▽ = 69 (Ga).

typical pyrolysis was conducted under argon for 4 h at 600 °C; however, the results were the same under an atmosphere of N_2 and even NH_3. The progress of the reaction was best be monitored by thermogravimetric analysis. The TGA (Figure 1) established that there was an abrupt weight loss at 150 °C followed by a smaller, broader weight loss at approximately 280 °C. The average of three runs yielded a value of 5.03% for the 150 °C event and an additional 1.80% lost by 500 °C at which point no further change was observed. The starting weight percent of hydrogen in the sample was 4.59%.

A study of the volatile products produced during the weight loss was conducted in a separate apparatus. Mass spectrometry was used to monitor the gases released as a function of temperature, and the results are shown in Figure 2. Despite the difference in heating rates of the TGA and mass spectrometry experiments, the temperatures of gas evolution corresponded to the weight loss events. Both NH_3 and H_2 were observed during the weight loss at 150 °C, but above this temperature only H_2 was evolved. A very small peak at $m/e = 69$ was observed which could be attributed to Ga. Because metallic gallium itself is involatile even at elevated temperatures, it is likely that this gallium

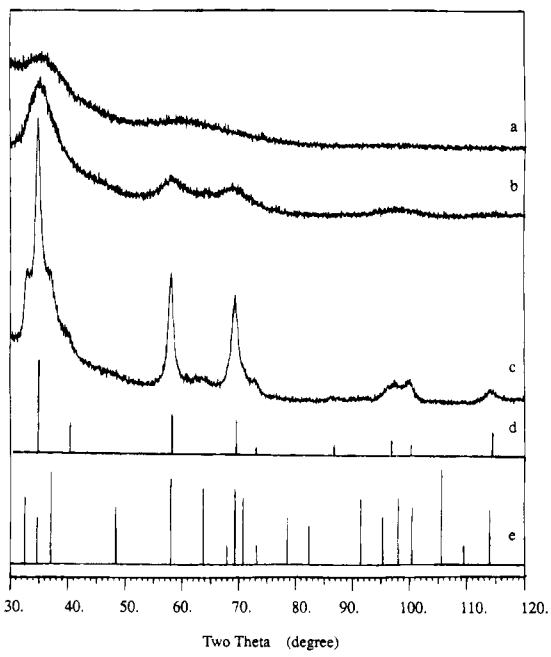

Figure 3. X-ray powder diffraction study of samples of cyclotrigallazane treated for four hours at 180 (a), 400 (b), and 600 °C (c). Pattern d is the calculated diffraction pattern for GaN assuming a zinc blende structure. Pattern e is the known diffraction pattern of *h*-GaN.

resulted from fragmentation of a small amount of cyclotrigallazane that sublimed during the pyrolysis under high vacuum. Independent mass spectral studies of $[H_2GaNH_2]_3$ established that the peak at $m/e = 69$ is one of the prominent fragments of this molecule.

Nitrogen analysis was performed on two samples from separate pyrolysis experiments, and the values (14.31 and 14.18%) were found to be in good agreement with each other. The values, however, were low compared to the calculated percentage of nitrogen in GaN (16.73%). On one of the samples, a complete analysis was performed and the results indicated that gallium accounted for the remaining mass. Values of potential impurities, carbon and hydrogen, were found to be below the detection limits (<0.5%). The percentages of Ga and N would correspond to the formulas $GaN_{0.83}$ or $Ga_{1.2}N$.

X-ray Powder Diffraction Results. Figure 3 shows a comparison of the powder diffraction data for samples of cyclotrigallazane treated at the stated temperature for 4 h. The powder was amorphous at 180 °C but became crystalline by 600 °C. On the basis of the Scherrer formula,[14] the coherence length of the solid treated at 600 °C was found to be 60 Å. The degree of crystallinity of samples treated for longer times at 600 °C did not change. Nor did changing the atmosphere from Ar to N_2 to NH_3 have any noticeable effect on the coherence length of the gallium nitride. Comparison of Figure 3c to 3e established that the GaN produced from the pyrolysis of cyclotrigallazane did not have the wurtzite structure. Indexing the reflections revealed the structure had a face-centered cubic lattice with a lattice constant of 4.50(2) Å. Careful inspection of Figure 3c revealed the presence of reflections at 32.5 and 37° possibly indicative of the presence of some hexagonal GaN. Using the model of a zinc blende structure, the intensities of the reflections were calculated and are shown in Figure 3d.

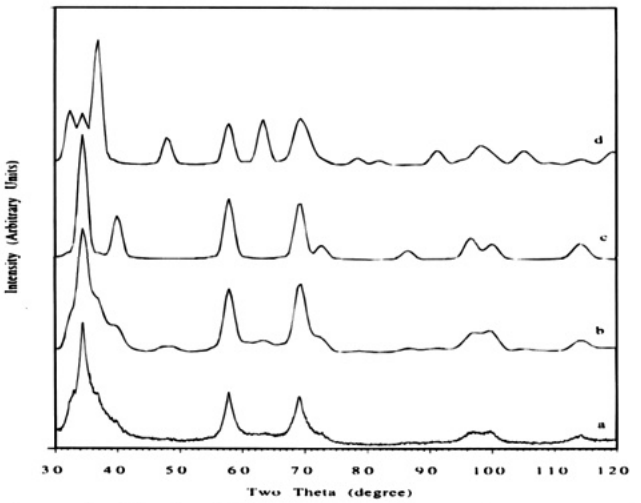

Figure 4. Simulated (for 60 Å particles) and experimental X-ray diffraction patterns: (a) experimental, (b) five stacking faults, (c) pure cubic particles, and (d) pure hexagonal particles.

Modeling X-ray Intensity Using the Debye Equation. The results of the calculated X-ray scattering for a purely hexagonal 60 Å particle (Figure 4d), a purely cubic 60 Å particle (Figure 4c) are compared to the experimental pattern (Figure 4a). A large number of discrepancies existed between the hexagonal and the experimental pattern whereas the cubic pattern seemed to be a better fit. The most notable problem with the cubic phase was the missing (200) and (400) reflections at 2θ values of 40.5 and 86.5° in the experimental pattern.

Patterns generated from physical mixtures of 60 Å particles of varying amounts of the pure cubic and pure hexagonal phases did not improve the fit to the data. Random or surface localized nitrogen vacancies had little impact of on the fits as did replacing all of the nitrogens on the outer 4.5 Å of the particle with gallium atoms. Some of the well-known[5,6] polytypes for compounds such as SiC and ZnS include packing arrangements such as ABCABACB- (8H). The calculated diffraction patterns for particles having these structures were closer to the experimental pattern. Calculations of patterns for particles with a basically hexagonal structure but containing 1 and 5 stacking faults established that only the latter gave a good fit (Figure 4b) to the experimental data. Five stacking faults within a 30-layer particle severely restricts order along the packing direction. To probe this issue further, we used a random number generator to create sequences of close-packed planes for 60 Å particles with no order along the packing direction. The results were similar to those shown in Figure 4b. The exact sequence of planes for the pattern shown in 4b is ABCACBACBACBABABA-BABCABABABABA and contains 46% hexagonal planes and 54% cubic planes. Each plane was identified as hexagonal or cubic by considering the neighboring planes. If the neighbors were the same, the plane in question was labeled hexagonal. Figure 4b displays a remarkable similarity to the experimental diffraction pattern. Increasing the percentage of cubic planes in the random sequences tended to reduce the intensity of the reflection located at 48°.

Transmission Electron Microscopy and Electron Diffraction. Two kinds of polycrystalline aggregates were observed in all samples taken for observation. One

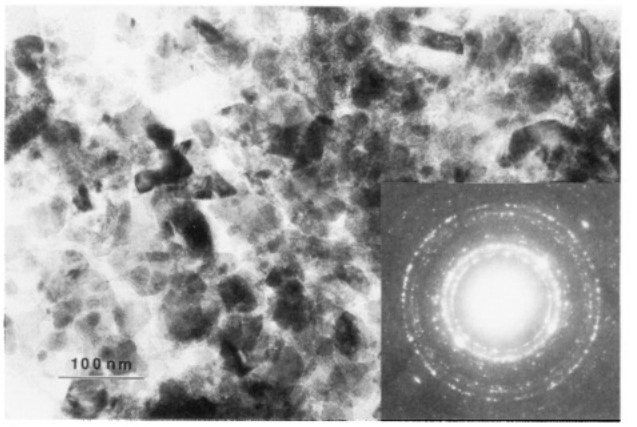

Figure 5. TEM image and electron diffraction pattern of microcrystals of *h*-GaN having well-developed facets.

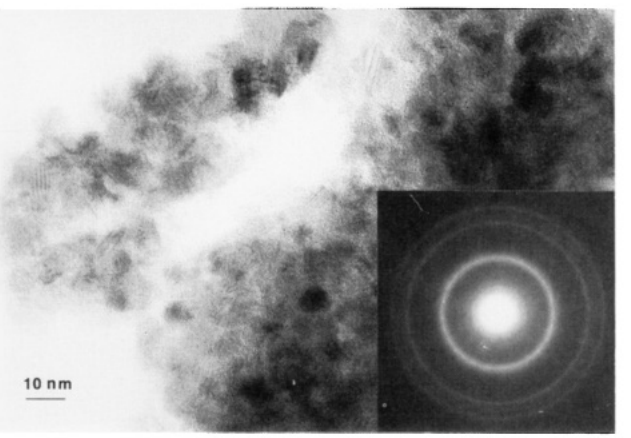

Figure 6. TEM image and electron diffraction pattern of nanocrystalline GaN.

set of aggregates consisted of microcrystals 200−1000 Å in size, with well-developed facets (Figure 5). Their diffraction patterns were composed of many distinct spots arranged in rings. Most of the rings could be indexed according to the known hexagonal GaN phase. The more abundant set of aggregates were comprised of much smaller crystals, up to 100 Å in diameter (Figure 6), and their diffraction patterns exhibited a set of seven continuous rings. An example of data found from measuring the ring diameters is shown in Table 1.

Only seven rings could be discerned on the negative of the diffraction pattern shown in Figure 6b. The three last ones had such a low intensity that they were difficult to print properly. As shown in Table 1, these diffraction rings could be indexed to a fcc structure having a lattice constant of 4.51(1) Å. The first and the fourth rings were broader than the others. Broadening of the first ring may have resulted from limited number of (111) planes in the numerous small crystals; an effect that could cause the already weak intensity of the (222) reflection to become undetectable. The broadening of the fourth ring resulted from near overlap of the (331) and (420) rings.

High-resolution micrographs show (111) lattice fringes in some nanocrystals which were properly oriented for observation (Figure 7).

Phase Transition Study. As stated above, continued heating of the *c*/*h*-GaN at 600 °C causes no further changes in the powder diffraction. Specifically, no

Table 1. Summary of Electron Diffraction Results for *c*-GaN

ring no.	ring diam[a] (mm)	D_n/D_1[b]	D_n^c/D_1^c[c]	fcc indices	d (Å)[d]	d^cGaN (Å)[e]
1	48.7 (br)	1	1	111	2.61	2.62
				200		
2	79.0	1.623	1.633	220	1.59	1.60
3	92.5	1.900	1.915	311	1.36	1.37
				222		
				400		
4	123.0 (br)	2.527	2.517	331	1.027	1.042
				420		
5	137.5	2.824	2.828	422	0.921	0.927
6	146.5	3.009	3.000	333	0.866	0.874
				440		
7	166.0	3.410	3.416	531	0.764	0.767

[a] Measured on an enlarged negative image. [b] D_n/D_1: ratios of the ring diameters. [c] D_n/D_1: ratios of the ring diameters calculated for the fcc structure. [d] Calculated from the calibrated camera length this gives a = 4.51(1) Å. [e] d spacings of *c*-GaN were calculated assuming a = 4.54 Å.[11]

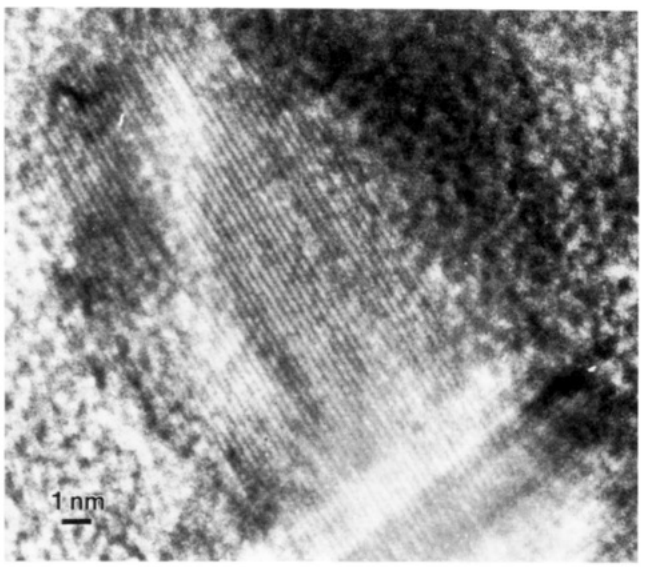

Figure 7. High-resolution TEM micrograph showing (111) lattice fringes in nanocrystalline GaN.

further crystallization of formation of hexagonal phase is observed. Figure 8 shows the powder diffraction results of a sample heated to 900 °C for a total of 120 h. Even with intermittent grinding of the sample, the phase transition was only 50% complete by this time. It is noteworthy that in addition to the phase change, the line widths of the reflections appeared to become sharper. This may indicate that some crystal growth is also occurring. More definitive statements are precluded due to the overlap of the reflections of cubic and hexagonal phases.

Alternative Preparations of *h*-GaN Powder and Thin Films. The reaction between NH_3 (1 atm) and Ga_2O_3 (eq 1) produces pure GaN in a matter of hours at 900 °C.[7] Repeating this procedure at 600 °C also produced GaN having the wurtzite structure; however, the conversion required over 300 h even with repeated grinding at intermittent times. Figure 9 shows the powder diffraction results at several points during the process. Even at the earliest stages, subtraction of the Ga_2O_3 pattern from the reaction mixture showed the three intense reflections, (110), (001), and (102), of the hexagonal phase in their appropriate relative intensities.

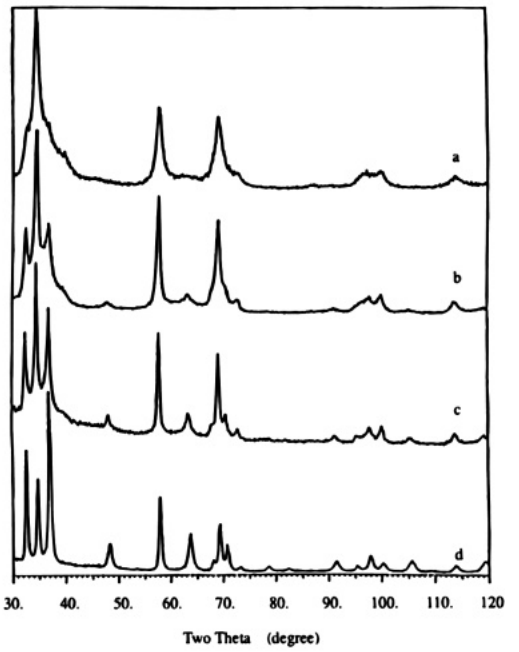

Figure 8. X-ray powder diffraction study of phase transition to *h*-GaN at 900 °C for 0 (a), 7 (b), and 122 h (c). Pattern d was obtained from a commercial sample of hexagonal GaN.

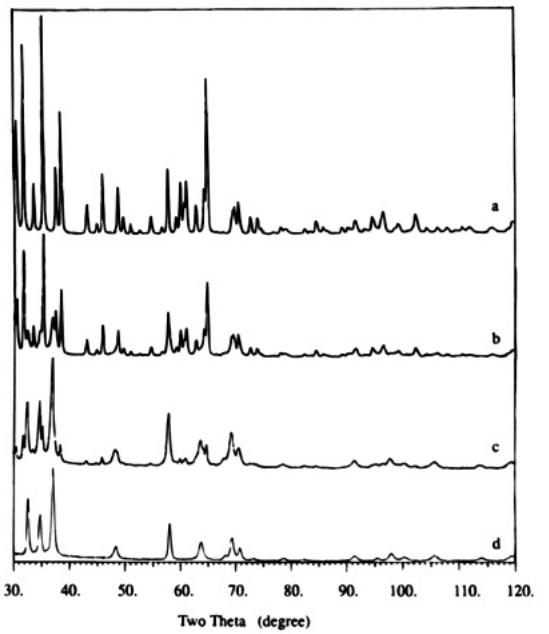

Figure 9. X-ray powder diffraction study of the progress of the reaction between Ga_2O_3 and NH_3 at 600 °C for 0 (a), 187 (b), and 305 h (c). At all stages, only *h*-GaN is observed. For comparison, pattern d was obtained from a commercial sample of hexagonal GaN.

The chemical vapor deposition of GaN was performed by subliming cyclotrigallazane from one end of a tube (held at approximately 45 °C) into a the region of the tube heated to 600 °C. A series of Si(100) wafers were placed in the hot zone toward the inlet (of $[H_2GaNH_2]_3$). The first wafers, which was at the lowest temperature, was not coated with a continuous film. The second and third wafers were both coated with an adherent, continuous film of GaN. The thicker coating, on the second wafer, was analyzed by X-ray diffraction, and the results (Figure 10) establish that film was polycrystalline GaN having the wurtzite structure.

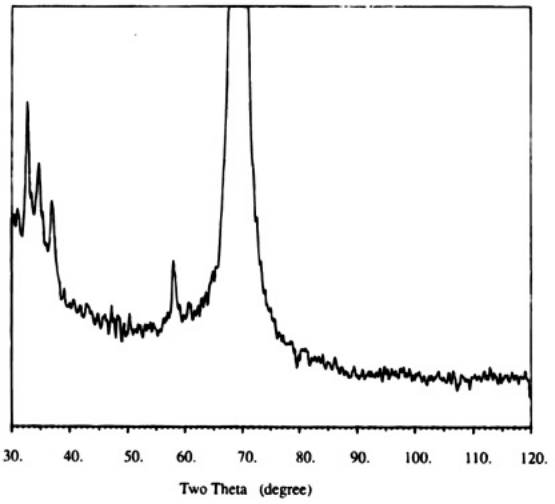

Figure 10. X-ray diffraction of the thin film of *h*-GaN on Si(100) prepared by the chemical vapor deposition using cyclotrigallazane.

Scheme 1. Summary of Experimental Transformations

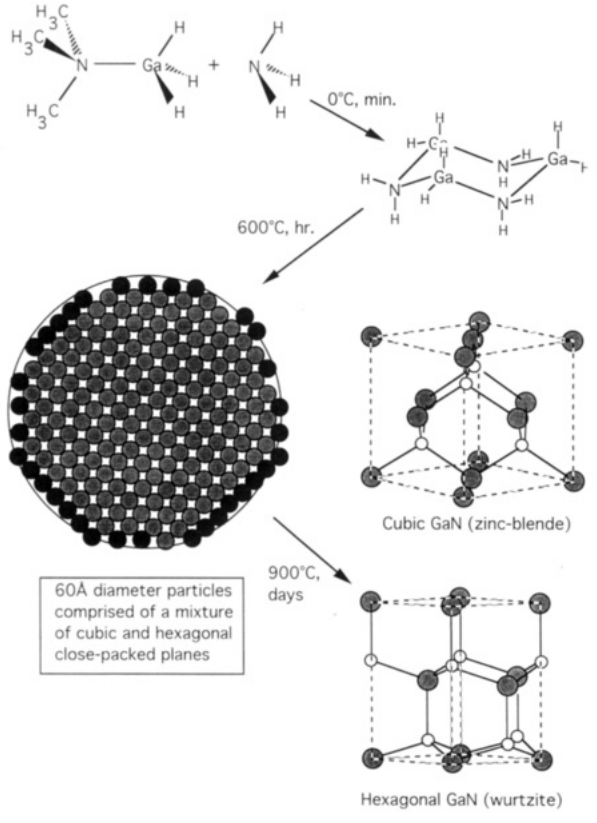

Discussion

A summary of the transformations observed during this study is shown in Scheme 1. The discussion will begin with comments on the structure and formula of the gallium nitride formed by pyrolysis of cyclotrigallazane. This will be followed by a discussion of the experiments designed to determine whether the structure of the solid formed during this pyrolysis is the result of kinetic or thermodynamic control of the reaction. The last section will focus on the relationship between the structure of cyclotrigallazane and *c*-GaN.

Nonstoichiometry. The elemental analyses performed on two independent preparations of nanocrystalline GaN powders gave the same results and establish that the overall ratio of gallium to nitrogen was not 1:1. This result alone cannot allow us to discriminate between a formula which is gallium rich ($Ga_{1+n}N$) or nitrogen poor (GaN_{1-x}). The average of three thermogravimetric analyses indicated an overall weight loss of 6.8% by 500 °C. Mass spectrometric measurements of the gases evolved during the pyrolysis of cyclotrigallazane in a vacuum chamber indicated the formation of hydrogen and ammonia corresponding to the first reaction at 150 °C. Only hydrogen was lost at temperatures greater than 150 °C. Weight loss from the sample during TGA would rule out $Ga_{1+n}N$ providing substantial amounts of sublimation did not accompany the weight loss events. During the first weight loss event the mass spectrometer detected small amounts of peaks having *m/e* of 69 which were attributed to gallium ions and indicative of some sublimation. The reproducibility of the TGA results and the involatility of cyclotrigallazane, however, suggest that only a very small amount of weight loss from sublimation could be contributing to the total loss of weight. Perhaps somewhat more convincing is the agreement between the formula calculated from the elemental analyses ($GaN_{0.83}$) with that calculated from the total weight loss assuming complete hydrogen and partial nitrogen loss ($GaN_{0.87}$).

Although deviations in stoichiometry of binary compounds are not uncommon, large (>10%) deviations from ideality are less routine. As summarized by Greenwood,[16] these deviations can manifest themselves structurally by one of the following four mechanisms: (1) quasi-random distribution of vacancies, (2) submicroheterogeneities (small domains of two or more compounds of differing stoichiometries), (3) ordering of the defects into a superlattice, and (4) formation of shear structures. In addition to these mechanisms for explaining the nonstoichiometry of bulk solids, differences between internal and surface stoichiometries can significantly affect the total stoichiometry for nanocrystalline materials.

Either of the two mechanisms involving an ordering of the defects, formation of a superlattice or collapse of the lattice to give a shear structure, would result in observable changes in both the X-ray and electron diffraction. That none are observed rules out these mechanisms. In examples of a large number of a quasi-random distribution of vacancies, changes (either positive or negative) in lattice constants are observed. Because *c*-GaN has not been previously characterized the ideal comparison of the nanocrystalline material produced from cyclotrigallazane cannot be made. We can, however, calculate a cubic unit-cell dimension based on the Ga–N bond distance (1.95 Å) obtained from the hexagonal structure.[17] The calculated value of 4.50 Å is, within experimental error, identical to the measured value of 4.51(1) Å. Both the estimated and experimental values of the cell dimension were slightly smaller than those reported for the thin films of *c*-GaN (4.52–4.55 Å).[10–12] For *h*-GaN, the effect of increasing the number of nitrogen vacancies was to decrease the lattice constants according to the approximate relation-

(16) Greenwood, N. N. *Ionic Crystals, Lattice Defects and Nonstoichiometry*; Butterworth: London, 1968; p 194.
(17) Juza, R.; Hahn, H. *Z. Anorg. Chem.* **1938**, *239*, 235.

Scheme 2. Effect of Surface Enrichment on Overall Stoichiometry

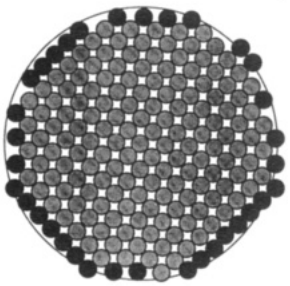

Number of atoms in the interior

$$n_{Ga(bulk)} = n_{N(bulk)} = 4\pi r^3 \rho N/3FW$$

r = radius
ρ = density of GaN
N = Avogadro's number
FW = formula weight of GaN

Number of Ga atoms on the surface

$$n_{Ga(surface)} = 4\pi r^2 \sigma$$

σ = surface area/Ga atom

Overall N/Ga

$$N/Ga = n_{N(bulk)}/[n_{Ga(bulk)} + n_{Ga(surface)}]$$

ship, $\Delta a/a = \Delta c/c = -V_N/N_{GaN}$,[18] where V_N represents the concentration (cm^{-3}) of N vacancies and N_{GaN} represents the concentration of GaN units (cm^{-3}). Although one would expect the change in lattice constants to saturate as the value of V_N increases, this relationship gives the direction and the sensitivity of the expected changes.

The fourth possibility, submicroheterogeneity, within the already small (60 Å diameter) nanocrystals seems unreasonable, unless we extend this concept to include differences between the surface and internal stoichiometry of the material. A simple mathematical model can be devised to assess the relative importance of the surface vs internal stoichiometries. The number of internal gallium and nitrogen atoms as a function of particle diameter can easily be calculated utilizing the density for bulk GaN and assuming spherical geometry of the particle. The number of surface atoms on this sphere can be estimated knowing the surface area and the size of each atoms' "footprint" on this surface (Scheme 2). For the purpose of the calculation we remove all of the nitrogen atoms from this surface layer and plot its effect on the overall N to Ga ratio as a function of particle diameter (Figure 11). The size of the gallium footprint was chosen as 7.94 $Å^2$; a number based on the magnitude of the Ga−Ga distance within the lattice of GaN (3.18 Å). The dotted line in the plot illustrates the sensitivity of the model to changing the size of the Ga footprint. The plus sign on Figure 11 shows the location of the GaN nanocrystals produced in this study. The graph demonstrates that for particles below 100 Å deviations of several tens of percent can be achieved and that one must be cautious in interpreting the results of any analytical procedure that gives results integrated over the entire particle.

We have been unable to devise any experiment that would give an unambiguous answer to the question of

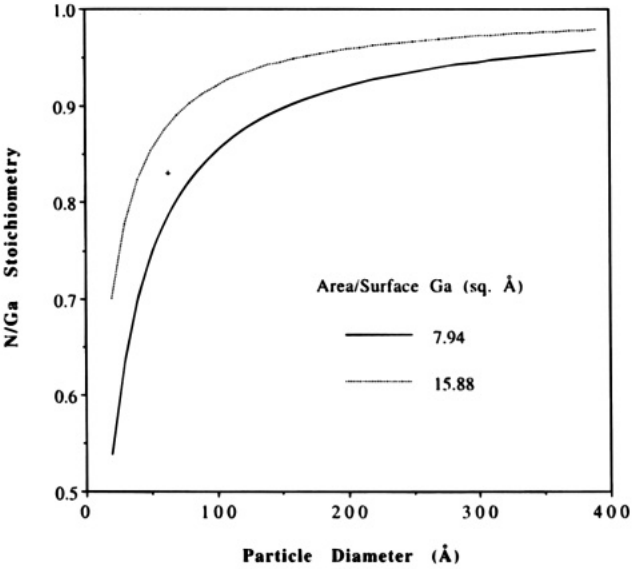

Figure 11. Results from the calculation probing the effect of differing stoichiometries between the surface and internal structure described in Scheme 2.

surface gallium enrichment. There are, however, several observations that could be explained by or are at least consistent with this picture. First, during the synthesis of the GaN nanocrystals ammonia was detected as a product during the first weight loss event at 150 °C. Although this mass spectral study was not quantitative, only a small signal due to Ga ions was observed. This suggests that a greater proportion of gallium compared to nitrogen remains on the sample. This protective coating could also contribute to our difficulty in growing larger crystals by heating for long periods at 600 °C. Taking this a step further, the reproducibility of the particle size from one run to the next, even under vastly different conditions, might be controlled in part by the buildup of gallium on the surface. These considerations suggest that eq 8 might more accurately represent the overall solid-state transformation.

$$[H_2GaNH_2]_3 \rightarrow GaN\ (83\%) + Ga\ (17\%) + NH_3 + H_2 \quad (8)$$

The last point to be made along these lines regards the gray to black color of these particles. Pure *h*-GaN has a pale yellow color. Numerous studies of nanocrystalline semiconductors have demonstrated that the bandgap increases with decreasing particle size.[19-21] The color of the GaN nanocrystals must result from some other effect.

Structure of *c*/*h*-GaN. Both the X-ray and electron diffraction results seemed to indicate that the solid had a well-developed, face-centered cubic lattice. The only significant deviation from ideality was that certain reflections, notably (200) and (400), were weaker than predicted (or essentially absent) for a zinc blende structure.

(18) Lagerstedt, O.; Monemar, B. *Phys. Rev. B* **1979**, *19*, 3064.

(19) Steigerwald, M. L.; Brus, L. E. *Annu. Rev. Mater. Sci.* **1989**, *19*, 471.
(20) Bawendi, M. G.; Steigerwald, M. L.; Brus, L. E. *Annu. Rev. Phys. Chem.* **1990**, *41*, 477.
(21) Murray, C. B.; Norris, D. J.; Bawendi, M. G. *J. Am. Chem. Soc.* **1993**, *115*, 8706.

In a study of the X-ray scattering of zinc blende and wurtzite CdSe nanocrystals, Bawendi and co-workers established[13] that for small particles (35–40 Å diameter) with a nominal spherical shape, the presence of stacking faults had a noticeable effect on the intensity of selected reflections. In particular, the presence of a relatively small number of stacking faults in a wurtzite lattice could cause the diffraction pattern to resemble that of the zinc blende structure. Other effects including compression or dilation of the lattice constant as a function of the radius, changes in the structure on the surface, and a capping of the particle with excess selenium caused little detectable change in the diffraction pattern. More recent studies showed that deviations from spherical shape also effect the peak shapes.[21]

The results of a similar analysis of the X-ray scattering of small particles of GaN are shown in Figure 4 along with the experimental spectrum. Although the scattering from the cubic phase was substantially closer to the experimental pattern, neither phase yielded a fully satisfactory fit to the data. We considered the scattering of many different structural models including specific polytypes, variation in the number of stacking faults and, ultimately, random packing sequences. The result shown in Figure 4b was obtained from a random packing sequence and exhibited the best fit to the experimental data among all the models. Further elaboration of the model either by (1) introducing random *N* vacancies at 17% of the sites throughout the particle, or by (2) introducing *N* vacancies localized on the outer 4.5 Å of the particle, or by (3) replacing all the nitrogens with galliums in the outer 4.5 Å of the particle had virtually no effect on the scattering pattern. We did not undertake a separate study of the effect of particle shape and size distribution. Although both of these are likely to effect the peak shapes, the studies on CdSe particles established that the presence and number of stacking faults dominated the appearance of the diffraction pattern. We conclude that the particles produced from the pyrolysis of cyclotrigallazane are a mixture of cubic and hexagonal close-packed layers.

Kinetic or Thermodynamic Control? Thus far we have presented evidence and arguments addressing the issue of the nature of the product of pyrolysis of $[H_2GaNH_2]_3$. In this section we will address the question of whether thermodynamic or kinetic factors control the formation of the random phase of GaN. It is possible that *c*/*h*-GaN is thermodynamically stable at 600 °C and that a phase transition exists somewhere between 600 and 900 °C (the temperature of most other syntheses). Alternatively, the pyrolysis of cyclotrigallazane could yield a kinetically trapped metastable phase.

The first experiment designed to differentiate between these was to attempt to observe the phase transition from *c*/*h*-GaN to *h*-GaN. At 600 °C no phase change was observed even after prolonged heating. This negative result does not answer the intended question because the kinetics of the phase transition may be too slow to observe. Indeed, even at 900 °C the phase change into *h*-GaN was only 50% complete after 120 h.

The second experiment involved repeating one of the original preparations of GaN at the lower temperature. The reaction of Ga_2O_3 with NH_3 (1 atm, eq 1) is complete within 1 h at 900 °C. At 600 °C, over 300 h (not including the time required to cool, grind, and reheat several times during the conversion) were required to achieve approximately 80% conversion. As seen in Figure 9, the product formed is *h*-GaN. Careful examination of the powder diffraction patterns at the early stages of this reaction also establish that *h*-GaN is formed. Because of the substantial reorganization that must take place in the lattice during this reaction, it seems unlikely that anything other than the most stable thermodynamic phase would result.

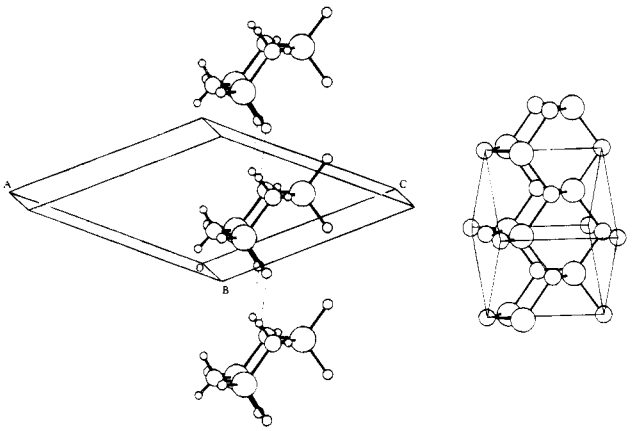

Figure 12. Relationship of the unit cell of cyclotrigallazane to the zinc blende structure.

In addition to these experiments, some results from the literature bear on this question. Polycrystalline films of *h*-GaN were produced at temperatures as low as 425 °C using $GaMe_3$ and N_2H_4 (eq 5). Bulk samples of aluminum nitride, which also exists in the wurtzite form, prepared using a high-temperature plasma torch reactor[22] exhibited evidence for the presence of a cubic phase. This observation is consistent with the fact that the high-temperature phase of boron nitride is cubic. Taken together these results establish that the thermodynamically stable phase of GaN at 600 °C is hexagonal. The random phase, therefore, is metastable at this temperature.

Topochemical Control of the Conversion of $[H_2GaNH_2]_3$ into *c*-GaN. The crystal structure of cyclotrigallazane is shown in Figure 12. The closest intermolecular contact between adjacent molecules is highlighted with dotted lines and involves a hydridic hydrogen on gallium and a protic hydrogen on nitrogen. The four atoms are nearly coplanar, but they are not collinear. The structural results were determined using a combination of single-crystal X-ray diffraction of $[H_2GaNH_2]_3$ and neutron powder diffraction of $[D_2GaND_2]_3$. The deuterium positions were refined for the neutron data using the Rietveld method.[23] The intermolecular D–D distance of 1.8 Å is closer than the van der Waals radii and suggestive of an attractive interaction. The dipolar nature of the Ga–H and N–H bonds is the probable cause of this attraction. Strong intermolecular bonding could explain both the involatility and insolubility of $[H_2GaNH_2]_3$ relative to gallazanes of similar and even higher molecular weights.

Figure 12 also highlights the topochemical relationship between the structure of cyclotrigallazane and the zinc blende structure. *By a series of "bimolecular"*

(22) Lu, Z. P.; Pfender, E. In *Ninth International Symposium on Plasma Chemistry*; Punochiuso, Italy, 1989; p 675.
(23) Hwang, J.-W.; Von Dreele, R.; Gladfelter, W. L., unpublished results.

hydrogen eliminations and Ga−N bond formations involving the closest intermolecular contacts, the essential architecture of the cubic gallium nitride structure would be established. We are not suggesting that a complete topotactic conversion of the micron-sized crystals of gallazane into *c*-GaN is occurring. The compression in unit cell volume from 62 Å^3/GaN unit in $[H_2GaNH_2]_3$ to 23 Å^3/GaN unit in *c*-GaN makes a topotactic reaction unlikely. Rather we propose that this solid-state topochemical reaction occurs creating nuclei throughout the crystal during the first stage of the transformation (corresponding to the weight loss event at 150 °C in the TGA studies). These nuclei lock in the cubic portions of the structure and subsequently grow to the 60 Å diameter nanocrystalline particles of *c*/*h*-GaN.

Hydrogen and alkane eliminations are common synthetic reactions in main-group organometallic chemistry. All of the gallazanes, including $[H_2GaNH_2]_3$,[1] and many related compounds of aluminum are prepared by reactions utilizing the anionic nature of a M−H or M−R group and the relatively acidic nature of the N−H group.[24] From solution studies, relatively little is known about the nature the bimolecular hydrogen elimination in main group compounds. On the basis of kinetic studies, the hypothesis has been presented that the elimination need not be intramolecular (i.e., the hydride[25,26] (or alkyl[27]) and the N−H reactants do not have to be coordinated to the same metal prior to the elimination event). Additional mechanistic studies on these widely used reactions would be valuable for understanding these transformations.

Three critical requirements for this topochemical conversion can be identified. *First, the molecular structure of $[H_2GaNH_2]_3$ has the correct formula, connectivity, and conformation so that when combined with the second feature, the packing of the molecules in the crystal structure, they resemble a significant portion of the zinc blende lattice. The third requirement is that there is a selective chemical reaction that retains this structural information during the solid-state polymerization.* One additional result confirms that removal of at least one of these requirements negates the formation of the cubic phase. Although the relatively involatile nature of $[H_2GaNH_2]_3$ would preclude its use as a reagent in typical chemical vapor deposition processing, we were able to grow thin films of polycrystalline GaN on silicon wafers. The cyclotrigallazane powder was placed in a tube near the entrance of the hot zone of a CVD reactor. The silicon wafers were placed closer to the gallazane in a region where the temperature was approximately 550 °C. X-ray diffraction measurements (Figure 10) established that the thin films formed were hexagonal GaN. The sublimation process destroys the relative positions of the molecules of $[H_2GaNH_2]_3$, and the surface mobility of the molecules or atoms on the growing GaN surface would favor the formation of the thermodynamically favored hexagonal phase.

As in all mechanistic studies, we cannot prove the mechanism of this chemical reaction. What has been presented is a series of relationships that are highly suggestive of a particular process leading to the first samples which are, in part, comprised of the previously unknown cubic phase of gallium nitride. Further, the insight gained by the study of this system may be valuable for designing new molecular routes to solid-state materials.

Acknowledgment. This work was sponsored by a grant from the National Science Foundation, the NSF Center for Interfacial Engineering, and the Minnesota Supercomputer Institute. We are grateful to Prof. David Kohlstedt and Dr. Quan Bai for their assistance with the experiment conducted at very high pressure and Professor Moungi Bawendi for a copy of his program for calculating scattering curves of small particles.

CM940418U

(24) Tuck, D. G. In *Comprehensive Organometallic Chemistry*; Wilkinson, G., Stone, F. G. A., Abel, E. W., Eds.; Pergamon: Oxford, 1982; Vol. 1, p 683.
(25) Beachley, O. T., Jr.; Tessier-Youngs, C. *Inorg. Chem.* **1979**, *18*, 3188.
(26) Beachley, O. T., Jr. *Inorg. Chem.* **1981**, *20*, 2825.
(27) Sauls, F. C.; Interrante, L. V.; Jiang, Z. *Inorg. Chem.* **1990**, *29*, 2989.